Available online at www.sciencedirect.com
ScienceDirect
International Journal of Mass Spectrometry 261 (2007) 146–151
International Journal of Mass Spectrometry
www.elsevier.com/locate/ijms

Electron impact ionization cross-sections of plasma relevant and astrophysical silicon compounds: SiH_4, Si_2H_6, $Si(CH_3)_4$, SiO, SiO_2, SiN and SiS

K.N. Joshipura [a,*], B.G. Vaishnav [b], Sumona Gangopadhyay [a]

[a] *Department of Physics, Sardar Patel University, Vallabh Vidyanagar 388120, Gujarat, India*
[b] *VPMP Polytechnic, Near Government ITI, Sector-15, Gandhinagar-382015, Gujarat, India.*

Received 20 July 2006; received in revised form 21 August 2006; accepted 22 August 2006
Available online 22 September 2006

Abstract

Total cross-sections (TCSs) for collisions of electrons having energies from ∼10 to 2000 eV are calculated for atomic silicon and its compounds SiH_4, Si_2H_6, $Si(CH_3)_4$, SiO, SiO_2, SiN and SiS, important in plasma and astrophysical applications. In each case total inelastic cross-sections are determined in the complex potential formalism and are partitioned into discrete and continuum excitation contributions in order to derive total ionization cross-sections. The present total (complete) cross-sections and total ionization cross-sections are found to be in a good general agreement with the previous data available for Si, SiH_4, Si_2H_6 and $Si(CH_3)_4$. This paper also reports the first theoretical ionization cross-sections for new targets SiO, SiO_2, SiN, and SiS for which almost no work of this kind has appeared in literature so far.

PACS: 34.80.Bm; 34.80.Dp

Keywords: Plasma relevant and astrophysical molecules; Silicon compounds; Total ionization cross-sections

1. Introduction

In recent decades, significant amount of research has been done on the theory of ionizing collisions of electrons with different atoms and molecules. Though the basic interactions between the colliding particles are known, the intractability of the resulting mathematical equations has led to useful approximations and methods of solutions. Several different approximate schemes have been developed to calculate reliably the total ionization cross-sections of mostly well-known and some exotic atomic–molecular targets so far [1–4]. Many of these targets have also been investigated experimentally. Most of the metal oxides we are interested in do not have a gas phase therefore there would be no experimental data. Besides, there is big list of molecules which are neither theoretically nor experimentally investigated so far.

Collisions of electrons with atomic silicon and its compounds find applications in different fields of research and industry, e.g., plasma physics and surface studies. Total cross-sections for electron impact ionization of the atomic targets like silicon are of great interest in discharges and plasmas as well as in gas lasers, planetary, cometary, and stellar atmospheres, radiation chemistry and mass spectrometry [5]. SiO is present in the photosphere of the sun and dust particles in the interstellar medium are composed mainly of silica (SiO_2), along with magnesium and iron silicates, amorphous carbon or water ice. The physics and chemistry of small translucent molecular clouds and the formation and identification of small diatomic molecules such as SiO, SiS and SiN in the interstellar medium have been discussed by Turner et al. [6] and Turner [7,8]. Among silicon bearing molecules, SiO is the most widespread there and it shows a large variation in abundance under varying physical conditions [6–8]. Silane (SiH_4) is an important molecule, detected on Saturn and on several other planets and their satellites. Cross-sections for the production of the silicon containing ions by electron collisional ionization of disilane Si_2H_6 is important for understanding the chemistry and

* Corresponding author.
E-mail address: knjoshipura@vahoo.com (K.N. Joshipura).

1387-3806/$ – see front matter © 2006 Elsevier B.V. All rights reserved.
doi:10.1016/j.ijms.2006.08.014

behavior of glow discharges in silane as used in the production of amorphous silicon thin films. Tetramethylsilane (TMS), i.e., $Si(CH_3)_4$ is the simplest organo-silane compound. It is a precursor in the plasma assisted chemical vapor deposition of SiN and SiC thin films and it is also an abundant reaction product in processing plasmas. TMS is utilized in plasma polymerization.

Among the present targets the tetrahedral SiH_4 is the only molecule for which a complete set of electron collisional data is available [9–12]. Total and partial ionization cross-sections for SiH_4 upon electron collisions are employed for the understanding and modeling of charge carrier balance in the plasma and the ion/radical chemistry in the gas phase as well as for the surface processes [5]. Atomic target Si and the molecular targets SiH_4, Si_2H_6 and $Si(CH_3)_4$ have been studied theoretically and experimentally. But, no data is available currently on electron impact ionization of SiO, SiO_2, SiN and SiS.

Our present interest is in the range of incident energy E_i from the threshold of ionization (∼10 eV) to 2000 eV. Therefore, total (*complete*) cross-section Q_T is the sum of total elastic cross-section Q_{el} and total inelastic cross-section Q_{inel}, i.e.,

$$Q_T(E_i) = Q_{el}(E_i) + Q_{inel}(E_i) \quad (1)$$

Experimental data on Q_T for well-known molecules like SiH_4 have been obtained by the Zecca–Karwasz group in Italy [10,11]. The electron impact ionization measurements are due to several other groups of workers [12,13]. Jiang et al. [14] calculated high energy Q_T for e-SiH_4 scattering.

Thus, the aim of the present paper is mainly to calculate total ionization cross-sections Q_{ion} for the targets listed in the title. The method employed for this purpose has been developed by us in recent years, viz., 'complex scattering potential-ionization contribution (CSP-*ic*) approach'. In this approach [15–19] we start with complex potential formalism to evaluate total inelastic cross-sections Q_{inel} and thereby deduce Q_{ion} under appropriate physical arguments. This theoretical method has been successful in a wide variety of atomic–molecular targets and hence the same has been used here as a predictive tool for the unknown targets SiO, SiO_2, SiN and SiS. We have used atomic units unless stated otherwise.

2. Theory

Details of the present theoretical approach are discussed in our earlier papers. At energies of the present interest the inelastic channels in electron–atom/molecule scattering consist of discrete excitations and ionizations, and this enables us to express the total inelastic cross-section as,

$$Q_{inel}(E_i) = \sum Q_{exc}(E_i) + Q_{ion}(E_i) \quad (2)$$

In this break-up, the first term is the sum over total *excitation* cross-sections for all accessible electronic transitions in the molecule, while the second term indicates the total cross-section of all allowed (single and multiple) ionization processes, with single ionization dominating at lower energies. The first term arises mainly from the low-lying dipole allowed transitions for which the cross-sections become small progressively above the ionization threshold. Hence, as the incident energy increases the second term in Eq. (2) dominates over the first, so that the calculated inelastic quantity Q_{inel} can be employed to derive the total ionization cross-section Q_{ion}. This theoretical approach, called the 'complex scattering potential-ionization contribution' or CSP-*ic* method, explores the advantages of the well-known complex potential representing simultaneous elastic and inelastic scattering. The complex potential $V(r, E_i) = V_R(r, E_t) + iV_I(r, E_i)$ has a real part V_R, consisting of static (V_{st}), exchange (V_{ex}) and polarization (V_{pol}) terms. The imaginary part also called the absorption potential V_{abs} is considered in the well-known quasi-free Pauli-blocking model of Staszewska et al. [20], after introducing a modification discussed below. This is an energy dependant potential that accounts for all possible inelastic scattering channels cumulatively, and has the generic form, in atomic units,

$$V_{abs}(r, E_i) = -\frac{1}{2}\rho(r)v_{loc}\sigma_{ee} = -\rho(r)\left(\frac{T_{loc}}{2}\right)^{1/2} \times \left(\frac{8\pi}{10k_F^3 E_i}\right)\theta(p^2 - k_F^2 - 2\Delta)(A_1 + A_2 + A_3) \quad (3)$$

Here v_{loc} is the local speed of the external electron, and σ_{ee} denotes the average cross-section of the binary collision of the external electron with one of the target electrons. The local kinetic energy of the incident electron is obtained from,

$$T_{loc} = E_i - V_R = E_i - (V_{st} + V_{ex})$$

In Eq. (3), $p^2 = 2E_i$, k_F the Fermi wave vector and Δ is an energy parameter. The Heaviside step-function $\theta(x)$ is such that $\theta(x) = 1$ for $x > 0$, and is zero otherwise. The dynamic functions A_1, A_2 and A_3, which are given in [20], depend differently on $\rho(r)$, I, Δ and E_i. The parameter Δ assumed to be fixed in the original model determines a threshold below which $V_{abs} = 0$, and the ionization or excitation is prevented energetically.

Improvements to overcome the shortcomings of this absorption model have been discussed by Blanco and Garcia [21], who have also suggested a variable form of Δ in order to account for screening effects of the target charge cloud on V_{abs}. The modification introduced in our papers [3,4,15,18,19] has been to assign a reasonable minimum value $0.8I$ to Δ and expressing this parameter as a function of E_i around I, as follows.

$$\Delta(E_i) = 0.8I + \beta(E_i - I) \quad (4)$$

where, E_p is the value of E_i at which the Q_{inel} attains maximum. In Eq. (4) β is obtained by requiring that $\Delta = I + 1$ (eV) at $E_i = E_p$, beyond which Δ is held constant. This expression for $\Delta(E_i)$ is meaningful since Δ fixed at I would not allow even excitation at incident energy $E_t = I$. On the other hand, if parameter Δ is much less than the ionization threshold, then V_{abs} becomes unduly high near the peak position. In short the present form of $\Delta(E_i)$, Eq. (4) balances all these aspects and allows us to obtain satisfactory values of Q_{ion} for a given target. The next step is to solve the Schrödinger equation with the modified V_{abs}, using the appropriate boundary conditions. Standard formulae [22] are used to generate Q_{inel} as well as Q_{el} by employing the complex phase shifts $\delta_l(k)$.

The inelastic cross-section Q_{inel} is not accessible directly in a single experiment, but in view of the Eq. (1), we have,

$$Q_{inel}(E_i) \geq Q_{ion}(E_i) \tag{5}$$

At incident energies above I, the ionization plays a dominant role due to the availability of infinitely many open channels of scattering. There is no rigorous way of projecting out Q_{ion} from the theoretical quantity Q_{inel}. Hence we have introduced an approximate procedure by defining a ratio,

$$R(E_i) = \frac{Q_{ion}(E_i)}{Q_{inel}(E_i)}, \quad 0 \leq R \leq 1 \tag{6}$$

Obviously $R=0$ when $E_i \leq I$. For a number of stable atomic–molecular targets like Ne, Ar, O_2, CH_4, H_2O, etc., for which the experimental cross-sections Q_{ion} are known accurately [23,24] the ratio R is seen to rise steadily as the energy increases above the threshold, and approaching unity at high energies. Thus,

$$R(E_i) = 0, \quad \text{for } E_i \leq I \tag{6a}$$

$$R(E_i) = R_p, \quad \text{at } E_i = E_p \tag{6b}$$

$$R(E_i) \cong 1, \quad \text{for } E_i > E_p \tag{6c}$$

Here, $R_p = 0.7$ stands for the value of R at $E_i = E_p$. The choice of this value is approximate but crucial. The peak position E_p (typically around 50 eV) occurs at an incident energy where the discrete excitation cross-sections are on the wane, while the ionization cross-section is rising fast, suggesting the R_p value to be above 0.5 but below 1. We follow the general observation [3,4,15–19,23,24] that at energies close to peak of ionization, the contribution of the cross-section Q_{ion} is about 70–80% in the total inelastic cross-section Q_{inel} and it increases with energy. This behavior of Q_{ion} is attributed to the fact that the important dipole allowed levels have thresholds below I and hence the fall of the first term $\sum Q_{exc}$ is faster than the first term in Eq. (1). Actually the R_p value, as also the function $R(E_i)$ itself depends on the location of low-lying dipole allowed energy levels with reference to the first continuum in a given target system, but for easily ionizable atoms and molecules (such as the present ones) having threshold I typically below 1 Rydberg (=13.6 eV) the present choice of R_p is found to be appropriate. Of course this approximation introduces an uncertainty in the calculated Q_{ion} but it is within the experimental uncertainties ~10–15%.

Now, for determining Q_{ion} from Q_{inel} we need R as a continuous function of energy $E_i = I$, hence we represent [15–19] the ratio $R(E_i)$ in the following manner.

$$R(E_i) = 1 - C_1 \left[\frac{C_2}{U + a} + \frac{\ln(U)}{U} \right] \tag{7}$$

Here U is the dimensionless variable

$$U = \frac{E_i}{I} \tag{8}$$

The particular functional form for $f(U)$ in Eq. (7) has also been explained in our earlier publications (e.g., ref. [3]). Eq. (7) involves dimensionless parameters C_1, C_2 and 'a', that reflect the target properties. The three conditions stated in Eq. (6a)–(6c) are used to determine these three parameters. To implement the third condition (6c) clearly, we first assume $a=0$ and consider a two-parameter expression in Eq. (7). Employing the two conditions (6a) and (6b) we first evaluate the C_1 and C_2. The resulting two-parameter expression is then used to obtain the value of R at a high energy $E_i = 10E_p$, and the same is employed in (6c).

Table 1
Ionization potentials and bond lengths of the present targets

Target	I (eV)	Bond length (Å)	
Si	8.15 [25]	–	–
SiH_4	11.65 [28]	Si—H	1.48 [25]
Si_2H_6	9.70 [28]	Si—H	1.49
		Si—Si	2.33 [25]
$Si(CH_3)_4$	9.80 [28]	Si—C	1.90
		C—H	1.10 [28]
SiO	11.43 [27]	Si—O	1.51 [25]
SiO_2	12.13 [27]	Si—O	1.53 [27]
SiN	11.74 [26]	Si—N	1.57 [26]
SiS	10.43 [26]	Si—S	1.93 [26]

Table 2
Present values of parameters E_p, C_1, C_2 and a

Target	E_p (eV)	C_1	C_2	a
Si	35	−1.102	−7.226	6.965
SiH_4	50	−1.643	−6.266	9.297
Si_2H_6	40	−0.805	−5.283	3.251
$Si(CH_3)_4$	50	−1.006	−7.517	6.563
SiO	45	−1.787	−7.585	12.552
SiO_2	60	−1.831	−8.200	14.018
SiN	70	−1.416	−9.195	12.021
SiS	60	−1.655	−8.769	13.510

The properties of interest, viz., ionization potentials and bond lengths of the present targets are adopted from the relevant literature [25–28] and are listed in Table 1. Next in Table 2 the present values of the parameters E_p, C_1, C_2 and a are exhibited for the present targets. In each case the energy parameter Δ is easily calculated from its analytical form, Eq. (6).

3. Results, discussions and conclusions

The theoretical approach CSP-*ic* outlined above offers the determination of the total cross-sections Q_T, Q_{el}, Q_{inel} and Q_{ion} along with a useful estimate on electronic excitations in terms of the summed cross-section $\sum Q_{exc}$. Although the present work covers all the major TCSs of electron impact on the present atomic and molecular targets, we have exhibited the more important cross-section Q_{ion} together with $\sum Q_{exc}$ for the lesser known molecules of the present list. Now for convenience we have organized the discussion of results into three subgroups of targets as follows.

3.1. Si and SiH_4

The calculated cross-sections along with compared data for electron scattering with Si atoms are exhibited in Fig. 1, where we have focused on ionization cross-sections in the main figure. Our present values of Q_{ion} agree very well with the theoretical data of DM calculations [29,30]. Fully orthogonalized first Born calculation of Bartlett and Stelbovics [31a,b] also shown here tends to overestimate in the peak region (around 30 eV), since the Born approximation is accurate only at high enough energies. Also, it does not make allowance for multiple ionization and autoionization processes and hence the Q_{ion} results of [31a,b] are seen (Fig. 1) to decay faster with energy beyond −200 eV. The said processes are included in our definition of Q_{inel} and Q_{ion}. However, all these theories including the present one differ from the only available experimental data of Freund et al. [32] in the position of the peak of Q_{ion}. The reason is that the present (and the other) calculations are based on the ionization potential $I = 8.15$ eV for Si atom, while in the experimental results of [32] the ionization signals begin to appear even below I, i.e., at 6 eV, as can be seen from their [32] Table V. The occurrence of ionization signal below the threshold can be traced back to a possible contamination in the atomic beam, say by a small amount of metastable excited Si atoms. This observation was also made by Bartlett and Stelbovics [31a,b], and by us in the case of Al atoms in [15]. Further in Fig. 1 we have also plotted the $\sum Q_{exc}$ which shows an estimate of the sum of the total excitation cross-sections for Si.

In Fig. 1 (inside box) we have plotted for future reference, the present values of Q_T and Q_{el} of e-Si scattering, although no comparable data exists in the current literature.

A more detailed comparison is possible in the case of e-SiH_4 scattering as shown in Fig. 2. The total (complete) cross-sections Q_T and the ionization cross-sections exhibited in this figure are from our earlier paper [3], but additional data are given presently. One can see a good accord of our Q_T results with the measured

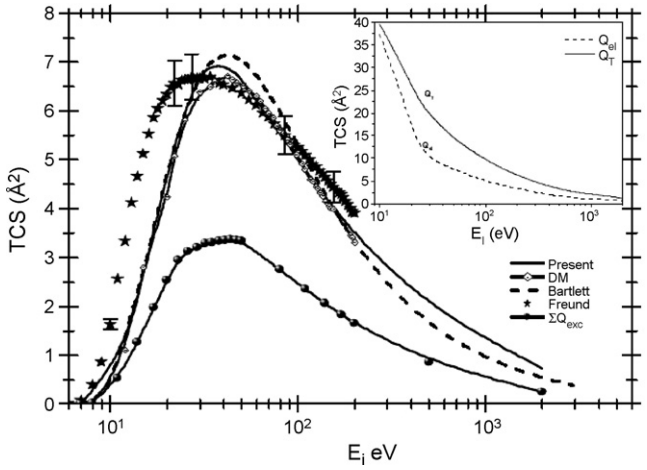

Fig. 1. Electron collisions with Si atom. Solid line present, Q_{ion}; solid line + diamond filled with dot, DM calculations [29,30] for Q_{ion}; dashed line, theoretical [31a,b] Q_{ion}; solid star, experimental [32] Q_{ion}. Lowest curve: solid line + sphere present, $\sum Q_{exc}$. Inside box: present, results, solid curve, Q_T, dashed curve, Q_{el}.

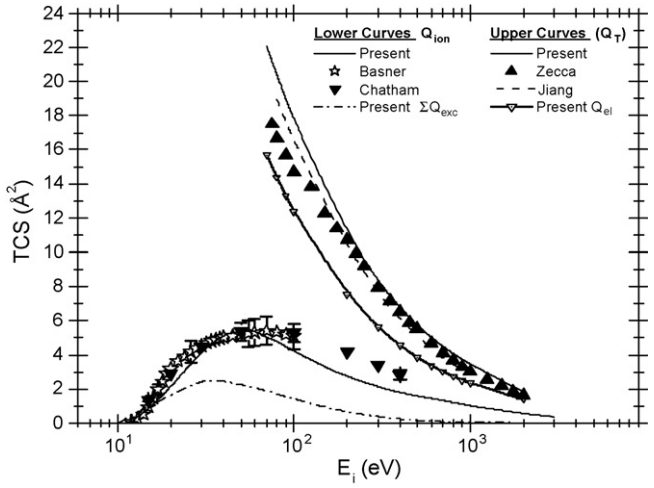

Fig. 2. Electron collisions with SiH_4. Upper curves: solid line present, Q_T; solid triangle, experimental [10,11] Q_T; dashed line, theoretical [14] Q_T; solid line + down triangle with dot present, Q_{el}. Lower curves: solid curve present, Q_{ion}; open star, experimental Basner et al. [9] Q_{ion}; solid down triangle, Chatham et al. [12] Q_{ion}. Lowest curve: present, $\sum Q_{exc}$.

data of Zecca et al. [10,11]. Also shown here are the calculations of Q_T by Jiang et al. [14] based on the high energy "addivity rule" (AR). Towards low energies the present values of Q_T are higher than the measurements of [11,24], in view of the limitations of the model potentials employed presently. Also plotted in Fig. 2 is Q_{el} for silane for which no comparison is available.

The present ionization cross-sections Q_{ion} of silane also match satisfactorily with the measured data of Basner et al. [9] as well as Chatham et al. [12]. The data of [9] showing a broad peak are reported only up to 100 eV. The present results decrease faster than the measured data-sets beyond the peak. The BEB theoretical data of Ali et al. [28], not shown, calculated with vertical ionization potential 12.7 eV of silane are found to be further lower than the present theoretical values. In several molecular targets the vertical and the adiabatic ionization potentials differ by about 1–2 eV [28] and this fact lends additional support for allowing the parameter Δ to vary as done presently.

The lowest curve in silane (Fig. 2) represents our theoretical values of the summed excitation cross-sections $\sum Q_{exc}$, for which again no comparison is available. It is difficult to ascertain the errors in the present values of $\sum Q_{exc}$, the sum over all allowed discrete excitation cross-sections. Some insight into this problem can be gained by recalling our similar results on methane molecule [3]. In [3] we compared the quantity $\sum Q_{exc}$ with the nearest available data, viz., electron impact neutral dissociation cross-sections of CH_4 measured with an error of about 35%. It is shown in [3] that our CSP-*ic* results agree with the said measurements. We may conclude as a guideline that the uncertainties in the present values of $\sum Q_{exc}$ could be around 35% or perhaps more.

3.2. Si_2H_6 and $Si(CH_3)_4$

For the exotic and important molecules disilane and TMS there is one previous data-set each for the theoretical as well

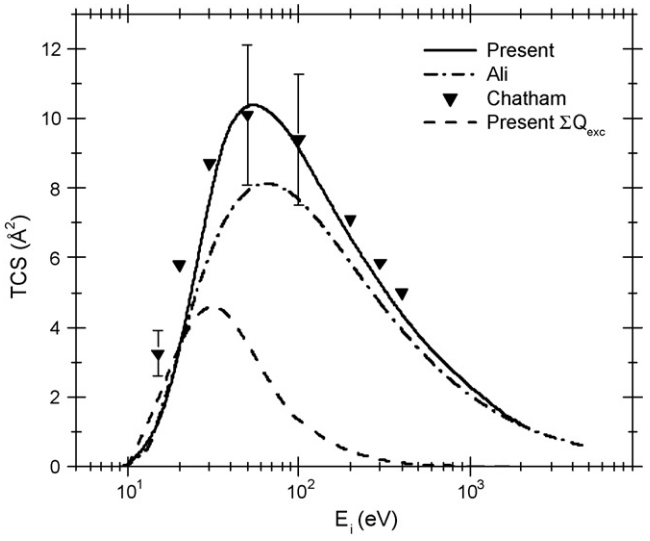

Fig. 3. Electron collisions with Si_2H_6. Solid line present, Q_{ion}; dashed dot line, BEB [28] Q_{ion}; solid down triangle, experimental [12] Q_{ion}. Lowest curve: present, $\sum Q_{exc}$.

as experimental results. Our calculated total ionization cross-sections along with compared data for these two targets are exhibited in Figs. 3 and 4, respectively. It is clear from Fig. 3 that the present Q_{ion} for Si_2H_6 are in a good accord with the measured data of Chatham et al. [12]. But the BEB values of Ali et al. [28] are on the lower side especially in the peak region. A large ionization cross-section is expected in the peak region, as obtained in our results, due to the large Si–Si bond length in disilane (Table 1).

The Q_{ion} of $Si(CH_3)_4$ are compared in Fig. 4 with the experimental data of Basner et al. [33], available only up to the peak of Q_{ion}, i.e., 100 eV. The BEB results of Ali et al. [28] are lower than the present and the measured values in this region. Since TMS is a big molecule having a relatively lower ionization threshold

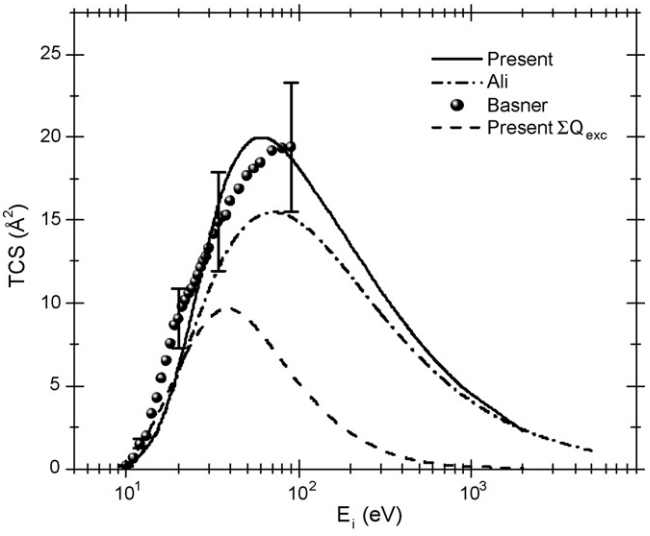

Fig. 4. Electron collisions with $Si(CH_3)_4$. Solid line present, Q_{ion}; dash dot line, BEB [28] Q_{ion}; solid sphere, experimental [33] Q_{ion}. Lowest curve: present, $\sum Q_{exc}$.

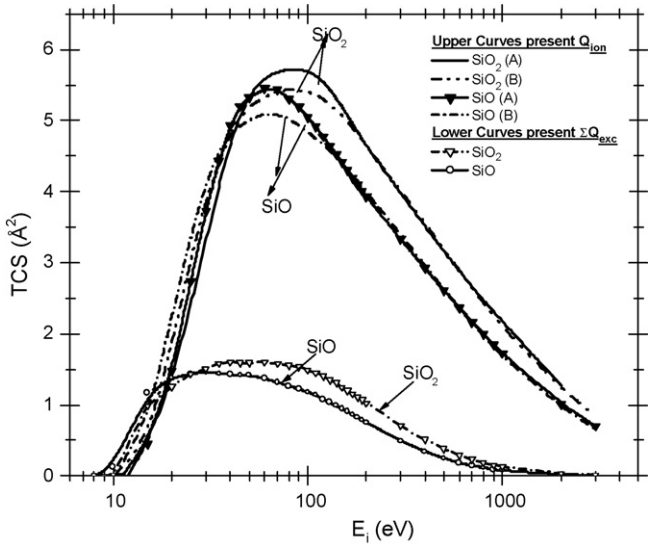

Fig. 5. Electron collisions with SiO and SiO_2, present A and B as in the text. Solid line + solid down triangle, SiO Q_{ion} (A); dotted line, SiO Q_{ion} (B), solid line, SiO_2 Q_{ion} (A); short dash dotted line, SiO_2 Q_{ion} (B). Lowest curves: solid line with open circle, SiO $\sum Q_{exc}$ (B); solid line with open down triangle, SiO_2 $\sum Q_{exc}$ (B).

(see Table 1) the Q_{ion} are expected to be high as indicated by our calculations.

The lowest curve each in Figs. 3 and 4 shows the present data for $\sum Q_{exc}$ in disilane and TMS, respectively.

3.3. SiO and SiO_2; SiN and SiS

SiO and SiO_2 are the important silicon oxides [26,27], comparable with the well-known molecules CO and CO_2, respectively. However, for the present oxides no electron scattering data are yet reported in literature, to our knowledge. We therefore restrict our presentation to the more important ionization and excitation cross-sections given in Figs. 5 and 6. The Q_{ion} for SiO and SiO_2 molecules shown in Fig. 5 are derived in two ways in order to gain a relative judgment. Thus, we calculated Q_{ion} for each of these targets by first taking a fixed value $\Delta = I$ (curve A) and then by varying Δ as per Eq. (4) (curve B). Of the two sets of data in each case in Fig. 5, the lower one is more reliable in view of our experience so far. Further, the SiO_2 cross-sections are somewhat higher than that of SiO, but the SiO peak lies towards lower energy, as understood easily from the target properties. The present quantities $\sum Q_{exc}$ corresponding to curves B serve to give an indication of electronic excitation processes in the targets, and these are exhibited by the two lowest curves in Fig. 5.

Finally, Fig. 6 represents the ionization and excitation cross-sections for the nitride and sulphide of silicon. Only one ionization curve is drawn in each case by the varying Δ method Eq. (4). The number of electrons in SiS is larger than in SiN, but the ionization threshold of the latter is slightly smaller (Table 1). This fact explains the peak positions and magnitudes of the two targets in Fig. 6. The SiO values (Fig. 5) are close to those of SiN (Fig. 6) as one would expect. The lowest curves in Fig. 6

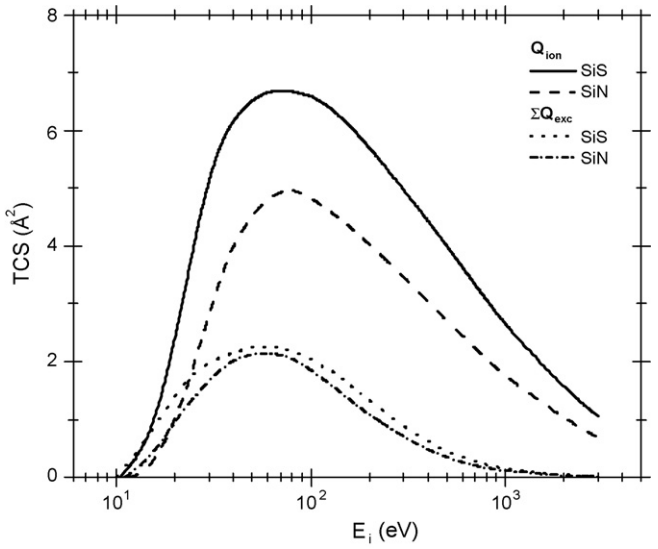

Fig. 6. Electron collisions with SiS and SiN present, results vide text. Solid line, SiS $Q_{ion;}$ dashed line, SiN Q_{ion}. Lowest curves: dotted line, SiS $\sum Q_{exc}$; dash dot dash line, SiN $\sum Q_{exc}$.

show the cumulative total excitation cross-sections $\sum Q_{exc}$ for SiS and SiN.

In conclusion we have presented in this paper our calculations on the different total cross-sections of electron scattering on Si atoms as well as their well-known and lesser known compounds. A good general agreement with the compared data sets is obtained here. Shortcomings of the present approximation arising in Eqs. (6) and (7) are also discussed appropriately. In the case of ionization of Si atoms (Fig. 1) our theory favours the other theories rather than the experimental results [32]. An interesting comparison of all the major cross-sections for the well-known silane targets is given by the bar chart in Fig. 7, showing the relative importance of different electron scattering processes. For the lesser known targets our aim has been to employ the CSP-*ic* method to predict the total ionization cross-sections together with the $\sum Q_{exc}$ contribution Therefore, we have reported presently the first data set for the lesser known molecules SiO, SiO_2, SiS and SiN, and these results will provide a meaningful reference for researchers in different fields.

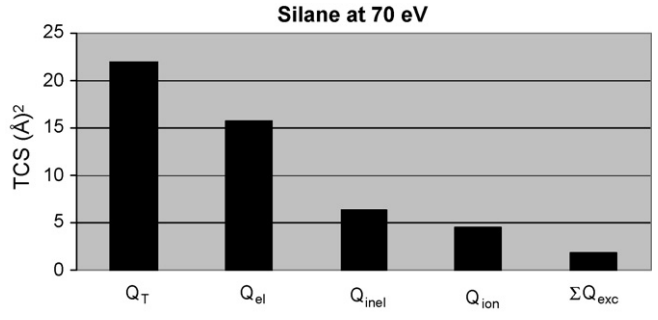

Fig. 7. Relative comparison of various total cross-sections for Silane at 70 eV.

Acknowledgement

This work was done as a part of research being carried out under a Project grant awarded to KNJ by Indian Space Research Organization, Bangalore, India

References

[1] H. Deutsch, K. Becker, S. Matt, T.D. Maerk, Int. J. Mass Spectrom. 197 (2000) 37, references therein.
[2] Y.-K. Kim, K.K. Irikura, M.E. Rudd, M.A. Ali, P.M. Stone J. Chang et al., From their NIST web-site http://physics.nist.gov/PhysRefData/Ionization/EII table.html.
[3] K.N. Joshipura, M. Vinodkumar, C.G. Limbachiya, B.K. Antony, Phys. Rev. A 69 (2004) 022705.
[4] Minaxi Vinodkumar, K.N. Joshipura, N.J. Mason, Phys. Rev. A, 74 (2006) 022721.
[5] I. Bray, A.T. Stelbovics, Adv. At. Mol. Opt. Phys. 35 (1995) 209.
[6] B.E. Turner, K.W. Chan, S. Green, D.A. Lubowich, Astrophys. J. 398 (1992) 114.
[7] B.E. Turner, Astrophys. J. 468 (1996) 694.
[8] B.E. Turner, Astrophys. J. 495 (1998) 804.
[9] R. Basner, M. Schmidt, V. Tarnovsky, K. Becker, H. Deustch, Int. J. Mass Spectrom. Ion Process. 171 (1997) 83.
[10] A. Zecca, G.P. Karwasz, R.S. Brusa, C.Z. Szmytkowski, J. Phys. B 24 (1991) 2747.
[11] A. Zecca, G.P. Karwasz, R.S. Brusa, C.Z. Szmytkowski, Phys. Rev. A 45 (1992) 2777.
[12] H. Chatham, D. Hills, R. Robertson, A. Gallagher, J. Chem. Phys. 81 (1984) 1770.
[13] V. Tarnovsky, H. Deutsch, K. Becker, J. Chem. Phys. 105 (1996) 6315.
[14] Y. Jiang, S. Jinfeng, W. Lide, Phys. Rev. A 52 (1995) 398.
[15] K.N. Joshipura, B.G. Vaishnav, C.G. Limbachiya, Pramana J. Phys. 66 (2006) 403.
[16] K.N. Joshipura, B.K. Antony, Phys. Lett. A 289 (2001) 323.
[17] K.N. Joshipura, C.G. Limbachiya, Int. J. Mass Spectrom. 216 (2002) 239.
[18] K.N. Joshipura, B.K. Antony, M. Vinodkumar, J. Phys. B: At. Mol. Opt. Phys. 35 (2002) 4211.
[19] K.N. Joshipura, M. Vinodkumar, B.K. Antony, N.J. Mason, Eur. Phys. J. D 23 (2003) 81.
[20] D. Staszewska, D.W. Schwenke, D. Thirumalai, D.G. Truhlar, Phys. Rev. A 29 (1984) 3078.
[21] F. Blanco, G. Garcia, Phys. Rev. A 67 (2003) 0022701, references therein.
[22] C.J. Joachain, Quantum Collision Theory, North Holland Press, Amsterdam, 1983, p. 110.
[23] G.P. Karwasz, R.S. Brusa, A. Zecca, La Rivista Del Nuovo Cimento 24 (2001) 1.
[24] A. Zecca, G.P. Karwasz, R.S. Brusa, La Rivista Del Nuovo Cimento 19 (1996) 1.
[25] R. Lide, CRC Handbook of Chemistry and Physics, CRC press LLC, Boca Raton, FL, 2003.
[26] S. Midda, A.K. Das, Eur. Phys J. D 27 (2003) 109.
[27] S.K. Nayak, B.K. Rao, S.N. Khanna, P. Jena, J. Chem. Phys. 109 (1998) 1245.
[28] M.A. Ali, Y.-K. Kim, W. Hwang, N.M. Weinberger, M.E. Rudd, J. Chem. Phys. 106 (1997) 1245.
[29] D. Margreiter, H. Deutsch, T.D. Märk, Int. J. Mass. Spectrom. Ion Process. 139 (1994) 127.
[30] H. Deutsch, K. Becker, T.D. Märk, Plasma Phys. Control. Fusion 40 (1998) 1721.
[31] (a) P.L. Bartlett, A.T. Stelbovics, Phys. Rev. A 66 (2002) 012707;
(b) P.L. Bartlett, A.T. Stelbovics, At. Data Nucl. Data Tables 86 (2004) 235.
[32] R.S. Freund, R.C. Wetzel, R.J. Shul, T.R. Hayes, Phys. Rev. A 41 (1990) 3575.
[33] R. Basner, R. Foest, M. Schmidt, F. Sigeneger, P. Kurunczi, K. Becker, H. Deutsch, Int. J. Mass. Spectrom. Ion Process. 153 (1996) 65.